Desalination and Water Treatment
www.deswater.com
51 (2013) 1004–1013
January
1944-3994/1944-3986
doi: 10.1080/19443994.2012.715131
Taylor & Francis
Taylor & Francis Group

Surface analysis for the identification of effective strategies to fight marine biofouling

Catharina Hippius, Stephan Nied*, Gregor Schürmann, Achim Feßenbecker

BASF SE, EV/WM - Water Solutions 67056 Ludwigshafen, Germany
Tel. +49 621 60 72897; Fax: +49 621 60 66 72897; email: stephan.nied@basf.com

Received 28 February 2012; Accepted 18 July 2012

ABSTRACT

Biofouling tremendously reduces performance of polymer membranes in desalination. The underlying processes involve multiple organisms and there is no complete picture of the involved interactions yet. Defined and reproducible testing strategies are therefore critically important in the successful development of effective cleaner systems. To address this need, we have introduced a two-stage approach to mimic the initial fouling process on membrane surfaces in contact with seawater. Based on thin films of membrane polymers, we established: (i) a molecular fouling model layer containing proteins, humic acids, and polysaccharidic substances and (ii) a bacterial layer of the marine micro-organism *Cobetia marina*. With our developed approach, we were able to quantify selectively both the stability of preadsorbed biomolecules and of attached micro-organisms and the extracellular polymeric substances (EPS) they secrete. Surface sensitive techniques including ellipsometry and various microscopy techniques (scanning electron microscopy, atomic force microscopy [AFM], and confocal laser scanning microscopy) were applied. Biofilm quantification and dissection of the different contributions of bacteria and matrix (EPS) to the film formation was achieved by fluorescence staining followed microscopic or spectroscopic analysis. After application of various cleaning agents, their efficiency to remove the fouling layer could be independently determined for both cellular and matrix components via a spectrofluorometeric plate reader technique, while high-resolution AFM studies revealed details on their cleaning mechanism. Exploiting this set of analytical methods, a combination of surfactant and protease could be identified as effective cleaning mixture that removed both bacterial cells and EPS under mild conditions. Conclusively, together with the advanced techniques for characterization, the established bacterial fouling layer could serve as a model system to screen for effective antifouling and cleaning strategies.

Keywords: RO membrane; Biofilm; Molecular and bacterial model fouling layer; Surfactant; Protease

1. Introduction

Marine biofouling results from the undesired deposition of micro-organisms, plants, algae, or animals on materials and devices in contact with biosystems and represents an ongoing problem affecting for example ship hulls, sensors, oceanographic instrumentation, aquaculture equipment, pipelines, and heat exchangers [1]. In the natural environment, biofouling

*Corresponding author.

Presented at the International Conference on Desalination for the Environment, Clean Water and Energy, European Desalination Society, 23–26 April 2012, Barcelona, Spain

occurs as a sequential process starting with the initial adsorption of organic macromolecules in dependence on the surface characteristics of the pristine material, the fluid composition, and the transport conditions at the interface [2–5]. Within the next step, the accumulated organic matter aids the subsequent colonization of the material by micro-organisms like bacteria, algae, fungi, and protozoa followed by the cellular deposition of extracellular polymeric substances (EPS) [6] composed of organics including polysaccharides, proteins, DNA, and RNA [7]. This resulting biofilm layer facilitates the attachment and growth of "macrofouling" species such as barnacles and tubeworms [6].

Biofouling on membranes used for water purification and wastewater reclamation is also one of the major concerns in reverse osmosis (RO) processes as it may decrease the system efficiency due to substantial flux decline and impaired salt rejection ability [7–9] caused by an increased overall hydraulic resistance for water permeation through the membrane and a hindered back diffusion of salts through the biofilm [10]. To combat these challenges, manufacturers undertake efforts to both prevent fouling formation and to effectively remove any accumulates from the membrane surface after a certain time of operation [8]. Based on that need, recently the basic interfacial processes causing the fouling of RO membranes and the propensity of different membrane materials to biofouling were explored [11–13]. Despite of the identification of the main constituents of the fouling layers being of colloidal, organic, bacterial, and of inorganic (mineral) origin, due to the complexity of the involved interactions [9], the development of effective antifouling and cleaning strategies remains demanding [8]. Although some substances were already tested for their potential to act as‚antifoulants' or‚cleaners' [14,15], for the screening process of such chemicals, defined but robust, rapid, and simple approaches are critically important.

To address this need, recently a reproducible, multicomponent early-stage molecular biofouling model layer was developed and immobilized on polyamide thin films as a representative membrane material commonly applied in RO processes [16]. These model films were based on polysaccharidic substances, proteins, and humic acids (HAs) thereby mimicking the initial biomolecular adsorption at membrane surfaces [17]. In experiments involving different classes of test substances (surfactants, acids, and chelating agents), utilizing ellipsometry to quantify layer thickness as read out, it could be clearly distinguished between the cleaning efficiency of these different agents. Moreover, this simple fouling model already allowed eliciting the underlying mechanism involved in binding/retention/release of fouling components. However, as the accumulation of organic substances on membrane surfaces only represents the starting point of the complex biofouling process, the use of representative microbiological systems involving species usually associated with biofilms could substantially increase the relevance of such model layers for the screening of antifouling or cleaning agents.

Therefore, in addition to the already implemented molecular fouling layers, a model system based on the common marine bacterium *Cobetia marina* (*C. marina*) [18] was established. These bacterial fouling layers were shown to be compatible with an array of powerful analytical methods for visualization and quantification of both cell and EPS contributions to the biofilm composition. Combining such defined model fouling layers and complementary analytical methods, the approach introduced here could be used to analyze the performance of various antifouling and cleaner systems, and to determine optimal conditions for their application.

2. Material and methods

2.1. Polyamide thin film preparation

Freshly cleaned planar silicon oxide carrier materials (silicon wafers 15 x 20 mm, GESIM, Germany or SiO_2-coated QCM-D crystals, Q-sense, Sweden) or glass slides (24×24 mm, Menzel-Gläser, Braunschweig, Germany) were oxidized in a mixture of aqueous ammonia solution (Acros Organics, Geel, Belgium) and hydrogen peroxide (Merck, Darmstadt, Germany) before they were subjected to hydrophobization with hexamethyldisilazane (ABCR, Karlsruhe, Germany). Subsequently, thin films of polyamide were immobilized applying spin coating from PA-12 solutions (VESTAMID, Evonik Industries, Germany). Solutions of 0.2% of VESTAMID were dissolved in hexafluoroisopropanol (Fluka, Germany) and subsequently spin coated at 3,000 rpm for 30 s (RC 5 Suess Microtec, Garching, Germany). The polyamide thin films showed a thickness of 19 ± 2 nm (ellipsometry, SE 400, Sentech, Berlin, Germany). The static contact angle of $76.3 \pm 1^\circ$ (OCA 30, Dataphysics, Filderstadt, Germany) confirms the hydrophobic characteristic of the films.

2.2. Multicomponent molecular fouling layers

2.2.1. Preparation of multicomponent molecular fouling layers

Preparation of molecular fouling layers was previously reported in [16]. Briefly, the model layers were

generated by directly covering the polyamide thin film substrate prepared on silicon oxide carrier materials with a solution of 0.25% alginate (AG; medium viscosity, Sigma-Aldrich), 200 ppm bovine serum albumin (BSA; Sigma-Aldrich) and 20 ppm humic acid (HA; Sigma-Aldrich). After 10 min adsorption, the excess liquid was removed by carefully tilting the wafers followed by a subsequent drying step at 60˚C for 5 min. The molecular fouling layers were stabilized by dipping them into a concentrated $CaCl_2$ (Merck) solution (8% [w/v]) for 10 s followed by an additional drying step at room temperature. This type of layers was used for all subsequent cleaning experiments. Prior to the cleaning experiments, all molecular fouling layers were dipped in MilliQ for 1 min and dried at room temperature. Resulting layer thickness was analyzed by ellipsometry.

2.2.2. Cleaning experiments with multicomponent molecular fouling layers

Selected cleaning conditions (alkaline pH) and agents (surfactants) were tested for their potential to decrease the thickness of multicomponent fouling layers as described previously [16]. Briefly, for cleaning at alkaline pH, 0.01 M NaOH (pH 12; Sigma-Aldrich) was used. The surfactants sodium dodecylbenzenesulfonate (LAS), surfactants A and B (BASF SE, Ludwigshafen, Germany) were dissolved in 0.01 M NaOH to an active concentration of 0.025%. The molecular fouling layers were immersed in aqueous solutions containing the selected agents for 10 min at room temperature followed by rinsing in MilliQ and drying at room temperature.

2.2.3. Quantification of cleaning efficiency by ellipsometry

According to the method reported previously [16], cleaning efficiency was determined by measuring the remaining layer thickness via a microfocus ellipsometer (Sentech SE-400, Sentech Instruments GmbH, Germany). Briefly, a wavelength of $\lambda = 632.8$ nm was used, while the angle of incidence was set to 65˚, 70˚, and 75˚. For further thickness measurements, a multilayer model was applied to calculate the thickness of the fouling layers and the underlying polyamid thin films. The refractive indices were: $n_{(Si)} = 3.858$; $n_{(SiO2)} = 1.4571$; $n_{(Polyamid)} = 1.47$; and $n_{(fouling\ layer)} = 1.47$. Cleaning efficiency was calculated according to the formula: cleaning efficiency = (1 – (remaining layer thickness/initial layer thickness) × 100%.

2.3. Bacterial fouling layers

2.3.1. Bacterial strain and growth conditions

To generate bacterial fouling layers, the marine bacterium *C. marina* (DSMZ4741) was used in this study. The strain was purchased from the DSMZ culture collections, Germany. Sea salt peptone (SSP, all ingredients purchased from Sigma-Aldrich) (sea salt 20 g; peptone 18 g; deionised water 1,000 ml, and pH 7.8) was used as the growth medium. The culture stock was maintained on sea salt peptone agar (SSPA, all ingredients purchased from Sigma-Aldrich) slants (sea salt 20 g; peptone 18 g; agar 30 g; deionised water 1,000 ml; and pH 7.8). Prior to the experiments, the culture was grown in the SSP medium on a rotary shaker at 180 rpm at 28˚C for 20–22 h in order to obtain cells in the logphase.

2.3.2. Preparation of bacterial fouling layers

The polyamid thin film substrates prepared on glass slides were conditioned for 24 h in artificial seawater (sea salt 20 g; deionised water 1,000 ml; and pH 7.8) before being transferred to the bacterial cell suspensions. A freshly grown (logphase) bacterial suspension was prepared with an absorbance of 0.2 at a wavelength of 600 nm (DU 800, Beckman Coulter, Krefeld, Germany). The conditioned replicate slides (four for each assay) were placed into individual compartments of quadric petri dishes and 5 ml of the bacterial suspension was added thereby fully immersing the slides. The plates were placed in an incubator at 28˚C on a rotary shaker (90 rpm). After 1 h of incubation, the slides were transferred into new quadric petri dishes containing 5 ml of fresh SSP medium. The plates were incubated for another 4 h at 28˚C on a rotary shaker (90 rpm) for the attached bacteria to proliferate on the surface of the slides. At the end of the incubation, the slides were gently rinsed in artificial seawater to remove any nonadherent cells.

2.3.3. Cleaning experiments with bacterial fouling layers

Similar to the experiments using the multicomponent molecular fouling layers, selected cleaning conditions (pH 12 and 10) and agents (LAS, surfactants A and B) were tested for their ability to remove bacterial cells and EPS matrix. Additionally, the cleaning potential of the protease subtilisin (Subtilisin A type VIII from Bacillus licheniformis, 12 U/mg, Sigma-Aldrich) applied alone or in combination with surfactant B was evaluated. For that, the enzyme (100 μg/ml) and/or surfactant B (active concentration

of 0.025%) were dissolved in 10 mM NaH_2PO_4 buffer (Sigma-Aldrich, pH 8.1). The bacterial fouling layers were immersed in the particular cleaning solution for 10 min at room temperature followed by rinsing in MilliQ. After that they were immediately fixed.

2.3.4. Fixation and staining

For fluorescence microscopy/spectroscopy and atomic force microscopy (AFM), bacterial fouling layers were fixed by transferring the respective slides into quadric petri dishes containing 4% paraformaldehyde (Sigma-Aldrich). After incubation for 15 min, the layers were rinsed with MilliQ and dried by nitrogen.

For fluorescence staining, the slides were placed into custom-made incubation chambers in order to avoid backside staining. To stain the EPS matrix, Alexa 488-conjugated Concanavalin A (Molecular Probes, distributed by Invitrogen, Netherlands) dissolved in 0.1 M sodium bicarbonate (Sigma-Aldrich) buffer (pH 8.3) was added for 1 h in the dark (25 μg/cm^2). After incubation, the solution was removed and samples were washed with phosphate buffered saline (PBS, Sigma-Aldrich) twice. For staining of bacterial cells, 4′,6-diamidino-2-phenylindole (DAPI) solution (dissolved in PBS) was applied to Concanavalin A-stained samples for 5 min in the dark (25 μg/cm^2). After removal of the solution, the layers were washed with MilliQ twice. Samples were taken out of the incubation chambers and dried by nitrogen.

For scanning electron microscopy (SEM), an alternative fixation procedure was performed to allow for optimized EPS visualization. Therefore, the samples were washed in PBS and fixed in 0.1 M cacodylate buffer pH 7.3 containing 2% paraformaldehyde, 2% glutaraldehyde, and 0.2% ruthenium red for 1hr at room temperature. Rinsing for 30 min in 0.1 M cacodylate buffer containing 7.5% sucrose and 0.1% ruthenium red was followed by postfixation in 0.1 M cacodylate buffer containing 1% osmiumtetroxide and 0.05% ruthenium red (all reagents Sigma, Germany; OsO4 by Roth, Germany). Next, the samples were washed in MilliQ and critical point dried (BAL-TEC CPD 030, Bal-Tec, Liechtenstein), sputtered with gold (Sputtercoater, BAL-TEC), and visualized using the FEI XL 30 scanning electron microscope.

2.3.5. Morphological analysis of bacterial fouling layers

After fixation, the morphology of the bacterial fouling layers was analyzed by microscopy. Fluorescently stained samples were evaluated by fluorescence microscopy (DMIRE2, Leica, Bensheim, Germany) using a 100x oil objective. Thereby, DAPI fluorescence was monitored with an excitation wavelength of 360 nm and an emission wavelength of 460 nm, while for Alexa 488-conjugated Concanavalin A, an excitation wavelength of 492 nm and an emission wavelength of 520 nm was used. Both images were combined to generate an overlay picture.

For analysis of the bacterial fouling layer morphology at a higher resolution, AFM and SEM were used. AFM imaging was performed on air dried samples using a JPK Nanowizard AFM (JPK Instruments, Germany) mounted on an Axiovert Observer D.1 inverted optical microscope (Zeiss, Germany). AFM cantilevers used had a nominal spring constant of 60 mN/m (SNL, Bruker). Feedback gains were optimized to get the best resolution of the topographs. Topographs were recorded at a line rate of 1.5 Hz in constant force contact mode, maintaining a contact force of $\geq$200 pN throughout the measurement. The SEM measurements were done on gold-coated samples utilizing an XL 30 ESEM (FEI, Netherlands) electron microscope in high-vacuum mode applying a voltage of 5–10 kV.

2.3.6. Quantification of cleaning efficiency by fluorescence spectroscopy

Fluorescently stained samples were placed into a custom-made slide holder. Fluorescence of DAPI and Alexa 488-conjugated Concanavalin A was measured in a plate reader (SPECTROFluor multiwell plate reader of TECAN GENios, Magellan software, Crailsheim, Germany) with the top mode using three flashes. The plate reader method was programmed to counterfeit the six-well flat bottom plates thereby resulting in a total number of 16 measurement points across each slide. The average number of these points was used to determine the relative bacterial biomass and EPS matrix attached to the surface after subtraction of the blank. As a blank, a polyamide slide was used, which had been exposed to the same conditions, but in the absence of bacteria. For evaluation of cleaning efficiency, the fluorescence intensity of the particular samples was compared to that of untreated slides thereby representing the originally deposited biofilm.

3. Results and discussion

Starting from the already established molecular model fouling layers composed of AG, BSA, and HA [16], we report a procedure performed to generate a bacterial fouling layer on polyamide thin films using the marine bacterium *C. marina*. Further on, methods for a thorough characterization of the resulting layer

are presented together with data obtained when analyzing the effect of various cleaner components to remove this fouling layer.

3.1. Preparation of bacterial fouling layers

Based on the method described by D'Souza et al. [19], bacterial fouling layers were prepared on polyamide films immersed in a culture of *C. marina* for a total time period of 5 h, in which the attachment, proliferation, and EPS deposition should occur. To prove the biofilm formation and to gain insights into the morphology of the resulting layers, several microscopical techniques were applied (Fig. 1).

For fluorescence microscopy, bacterial cells were visualized by DAPI-staining of their DNA, while the EPS was stained by the Alexa 488-conjugated lectin Concanavalin A, which selectively binds to α-mannopyranosyl and α-glucopyranosyl residues in EPS [20]. Fig. 1 (left) shows that the resulting biofilm prepared on polyamide surfaces consists of both bacterial cells and EPS. The matrix thereby fills the intercellular space, while larger deposits were also found on top of the bacterial layer. As an advantage of this technique, fluorescence microscopy requires only minimal sample preparation. Besides the fact that it enables the researcher to analyze the micro-organism itself, it also permits studying the surrounding environment. Here, not only the localization of the EPS could be visualized, but selective staining additionally allows to draw conclusions about the nature of the matrix, which consists in the case of *C. marina* of polysaccharides with α-mannopyranosyl and α-glucopyranosyl residues.

Despite these advantages, to further analyze the biofilm at a higher resolution, AFM was applied. This technique can be used to perform real-time, high-resolution imaging of the bacterial fouling layer in three dimensions. Moreover, there is no need of preimaging treatments such as staining that might affect biofilm morphology. Fig. 1 (middle) shows a representative image of the model fouling layer taken by AFM. At such high resolution, an oval cell morphology of *C. marina* could be visualized. The cell shape found here correlates with the description of this gram-negative bacterium, which transforms from a coccoid shape in the stationary growth phase to a rather elongated morphology as the cells proliferate [21]. Moreover, also by AFM imaging, deposits of EPS (white arrows in Fig. 1, middle) on top of the cellular layer could be detected.

For an even more advanced imaging of the biofilm, SEM was used. The advantage of SEM is its ability to examine and analyze specimens, including bacteria, at magnifications up to 500,000×. However, as a disadvantage, biological samples usually have to be covered by an electrically conducting coating, while this process could alter or destroy the morphology of specimen. Therefore, for visualization via SEM, the biofilms were treated by a special procedure. This protocol involves fixing the fouling layer by glutaraldehyde, which attaches the biofilm on the polyamide surface more effectively. Cacodylate was used to remove any interfering residuals such as salts, while osmium tetroxide substantially enhances the contrast. Moreover, ruthenium red interacts with carbohydrates of the EPS, which makes it possible to visualize the

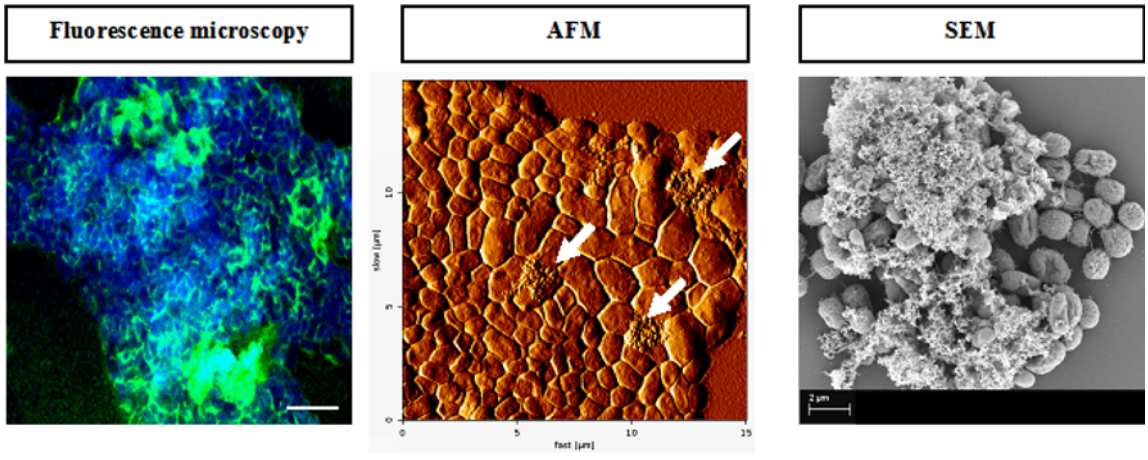

Fig. 1. Morphological analysis of bacterial model fouling layers prepared on polyamide film. Images clearly show the biofilm being composed of bacterial cells and EPS. Left: image taken by fluorescence microscopy; bacterial cells were stained by DAPI (dark gray), while Concanavalin A-staining (light gray) was used to visualize the EPS matrix (bar: 10 μm). Middle: image taken by AFM; arrows point at the deposition of EPS. Right: image taken by SEM; the biofilm was fixed by a special procedure to facilitate visualization of the EPS structure.

matrix and which enhances the resolution [22]. Applying this procedure (Fig. 1, right), both bacterial cells as well as large deposits of the EPS could be imaged by SEM. Once again, the oval shape of *C. marina* was validated. At such high resolution, it was also found that the cellular dimensions of the bacterium were in the range of 0.6–1.2 μm × 1–4 μm as it was reported by Cobet et al. [21]. Moreover, with this advanced imaging technique, also structural details of the EPS could be resolved.

Taken together, the successful formation of a *C. marina* biofilm on polyamide surfaces was proven by several microscopical techniques. By the combination of fluorescence microscopy, AFM, and SEM, the morphology of the fouling layers composed of bacterial cells and EPS could be analyzed, while detailed structural information were obtained.

3.2. Cleaning experiments to remove bacterial fouling layers

To evaluate the suitability of the established bacterial fouling layers for an application as main readout to dissect cleaning efficiency and underlying anchoring mechanism of biofilm components, there is a need for a precise method to quantify the biofilm on the polyamide surfaces. For that, the spectrofluorometeric plate reader technique described by D'Souza et al. [19] was applied. However, by an evaluation of the double fluorescence staining with DAPI and Concanavalin A, it is additionally possible to distinguish between bacterial cells and EPS deposits on the polyamide film. With this technique, the cleaning efficiency of specific washing procedures and cleaning substances can be individually determined for both biofilm constituents.

Fig. 2 shows the results of cleaning experiments performed with MilliQ (pH 12 or pH 10; control to exclude cleaning effects of alkaline pH), LAS as well as two model surfactants termed surfactants A and B (dissolved in MilliQ pH 12 or 10). For a comparison of the data obtained for bacterial (Fig. 2(B) and (C)) fouling layers, once again the cleaning efficiencies of the different agents determined with the already established molecular fouling layers composed of AG, BSA, and HA [16] are displayed in Fig. 2(A). Here, a simple application of MilliQ pH 12 was not able to remove these molecular fouling layers, while LAS also could not detach significant parts of it (∼1%). In contrast, both surfactants A and B revealed a high cleaning efficiency (∼90 and 95%, respectively).

Interestingly, using the same standard pH conditions (pH 12), similar results could be obtained with the bacterial fouling layers (Fig. 2(B)) when considering the cleaning effect on both bacterial cells and EPS. While MilliQ pH 12 did not enable a reduction of the biofilm, Surfactant A (∼50% bacteria; 15% matrix) and Surfactant B (∼50% bacteria; 10% matrix) removed substantial quantities of the bacterial fouling layers. In this setting, also LAS displayed a significant cleaning efficiency (∼35% bacteria; 10% matrix); however, when considering the removal of the bacterial cells, it did not perform equally well as surfactants A and B thereby confirming the results obtained with molecular fouling layers. Remarkably, no such trend was obtained for the detachment of EPS. However, this might be due to the fact that overall only small quantities of the EPS could be removed by a surfactant treatment at all indicating that such cleaning might be not sufficient for releasing the bacterial matrix from RO membranes.

In order to clearly distinguish between the performances of different cleaning agents as well as to analyze the possibility for their application under milder conditions, cleaning experiments using bacterial fouling layers were additionally performed at different pH conditions (pH 10, Fig. 2(C)). As expected, once again slightly alkaline MilliQ (pH 10) was not able to detach the biofilm. However, the milder pH conditions also decreased the cleaning efficiency of LAS and Surfactant A. Surfactant A removed at least both bacteria and matrix (∼20% bacteria; 10% matrix); LAS could only release small quantities of bacteria (∼10%), but no EPS. Interestingly, the cleaning efficiency of Surfactant B at pH 10 (∼60% bacteria; 20% matrix) was at minimum equally high as at pH 12, thereby indicating that this substance might represent the only surfactant tested here, which could be applied under milder conditions without affecting its performance.

In summary, similarities between the results of cleaning experiment performed with molecular and bacterial fouling layers show that both systems might represent relevant models for early-stage biofouling films. Moreover, with the established bacterial fouling layers and the respective analytical techniques presented here, it is possible to clearly differentiate between the performance of several cleaning agents for both bacterial cells and EPS matrix, thereby underlining the advantages of the current approach.

As a treatment with surfactants results in the removal of substantial quantities of bacterial fouling layers, it might be interesting to additionally evaluate potential changes in the biofilm morphology. Although fluorescence microscopy (Fig. 2(B) and (C)) could be used to get an overview about the general distribution of bacterial cells and EPS after the cleaning procedures, imaging via high-resolution techniques such as AFM might provide further structural details. Fig. 3 shows the evaluation of the bacterial

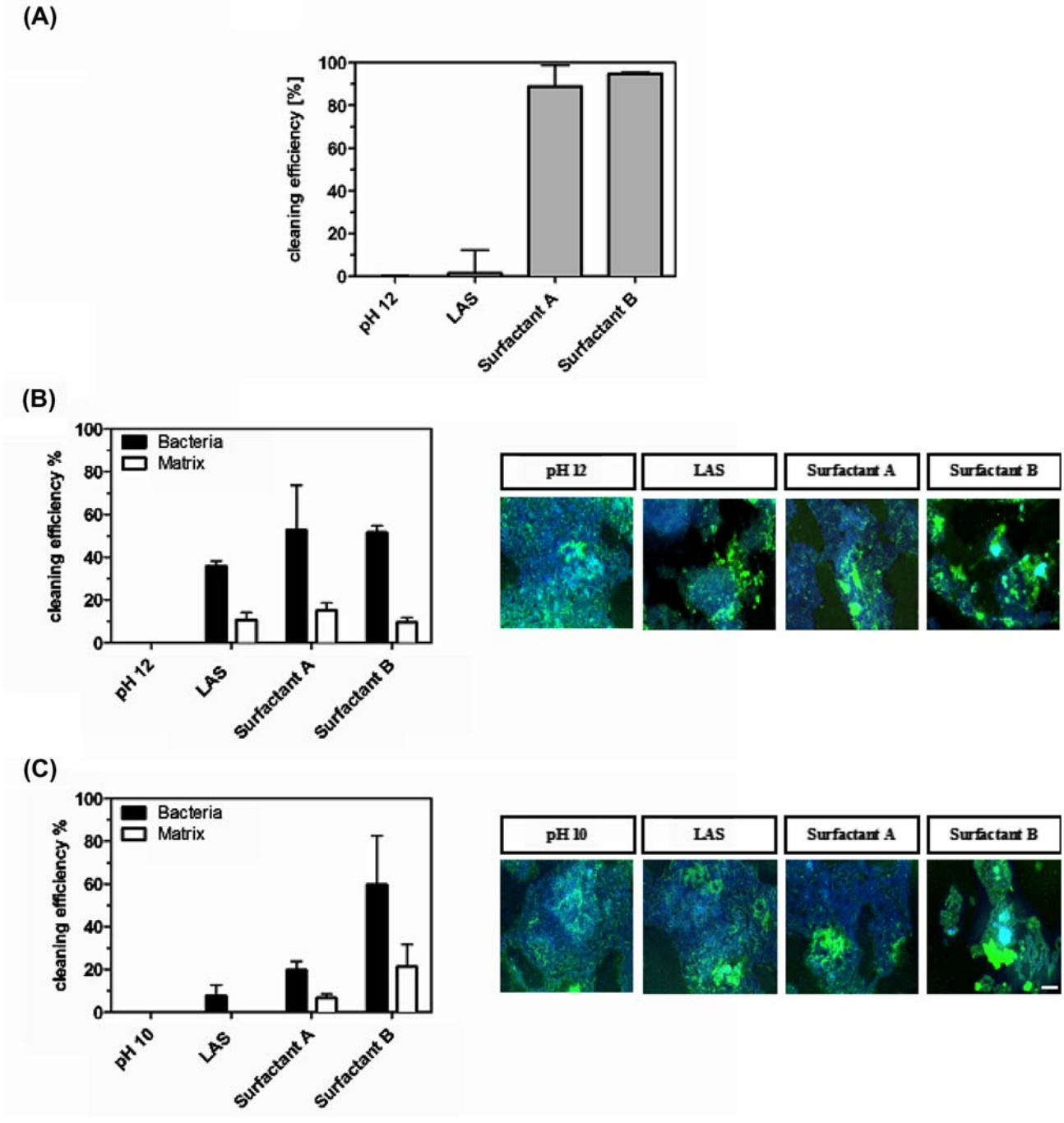

Fig. 2. Results of cleaning experiments performed with molecular (A) or bacterial (B and C) model fouling layers. A: quantification of the cleaning efficiency for MilliQ pH 12, LAS, Surfactant A, and B (all surfactants dissolved in MilliQ pH 12) applied to molecular model fouling layers. B: quantification of the cleaning efficiency for MilliQ pH 12, LAS, Surfactant A, and B (all surfactants dissolved in MilliQ pH 12) applied to bacterial model fouling layers (left) and respective fluorescence microscopy images (right). C: quantification of the cleaning efficiency for MilliQ pH 10, LAS, Surfactant A, and B (all surfactants dissolved in MilliQ pH 10) applied to bacterial model fouling layers (left) and respective fluorescence microscopy images (right). Bacterial cells were stained by DAPI (dark gray), while Concanavalin A-staining (light gray) was used to visualize the EPS matrix (bar: 10 μm).

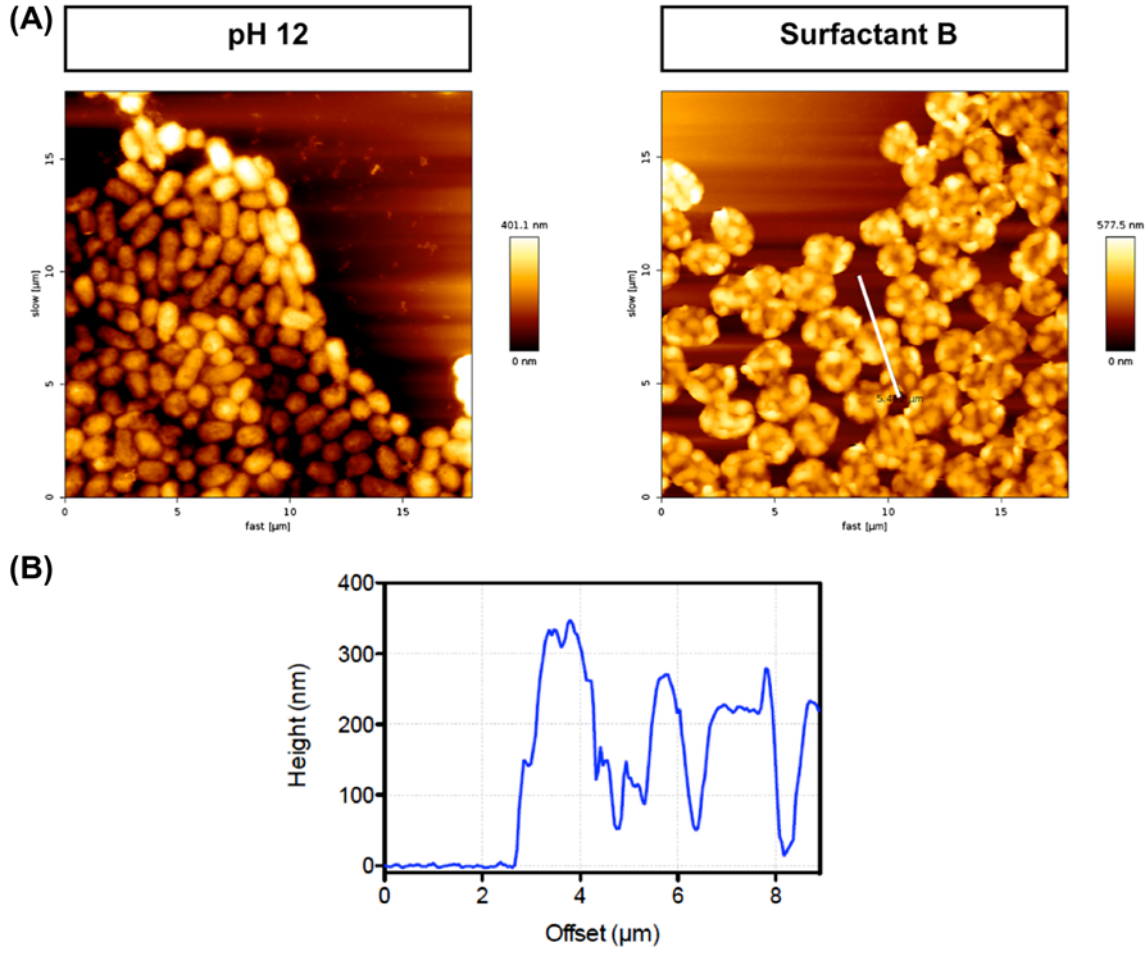

Fig. 3. Evaluation of bacterial fouling layer morphology via AFM in dependence on the cleaning conditions. A (left and right): images of biofilms treated with MilliQ (pH 12) and Surfactant B (dissolved in MilliQ pH 12). B: height profile of the bacterial fouling layer treated with Surfactant B. The profile was determined for the distance illustrated in A (right, white line).

fouling layer morphology via AFM in dependence on the cleaning conditions. Considering the general appearance of the cell shape (Fig. 3(A)), a simple alkaline treatment with MilliQ pH 12 (right) does not alter the general biofilm morphology (for comparison, see Fig. 1, middle). However, after application of Surfactant B (left), cells start to successively detach from the polyamide films as indicated by the "buckling" of their surface.

This effect could be verified by the determination of the biofilm height profile (Fig. 3(B), measured for distance illustrated in Fig. 3(B), right, white line). Here, as the AFM cantilever touches a bacterium (at an offset of ~2.5 µm), the irregular pattern is caused by cell areas that are still closely attached to the polyamide surface (corresponding to height minima of ~80 nm) as well as by areas, which already come off the substrate (corresponding to height maxima of up to ~350 nm). Compared to the smooth and regular profile determined for untreated biofilms with cells of ~80 nm and EPS cluster with ~200 nm height (data not shown), these results clearly demonstrate that Surfactant B exerts its cleaning effect by facilitating the detachment of bacterial cells.

Taken together, using high-resolution AFM, changes in the morphology of bacterial fouling layers after cleaning treatments could be unraveled. Therefore, such studies provide first insights into the underlying cleaning mechanism exerted by a particular substance.

After analyzing the ability of surfactants to remove substantial quantities of the cellular part within biofilms, it should be evaluated whether other classes of cleaning agents as well as mixtures of different substances might be applicable to especially release the EPS matrix more effectively. Fig. 4 shows the results

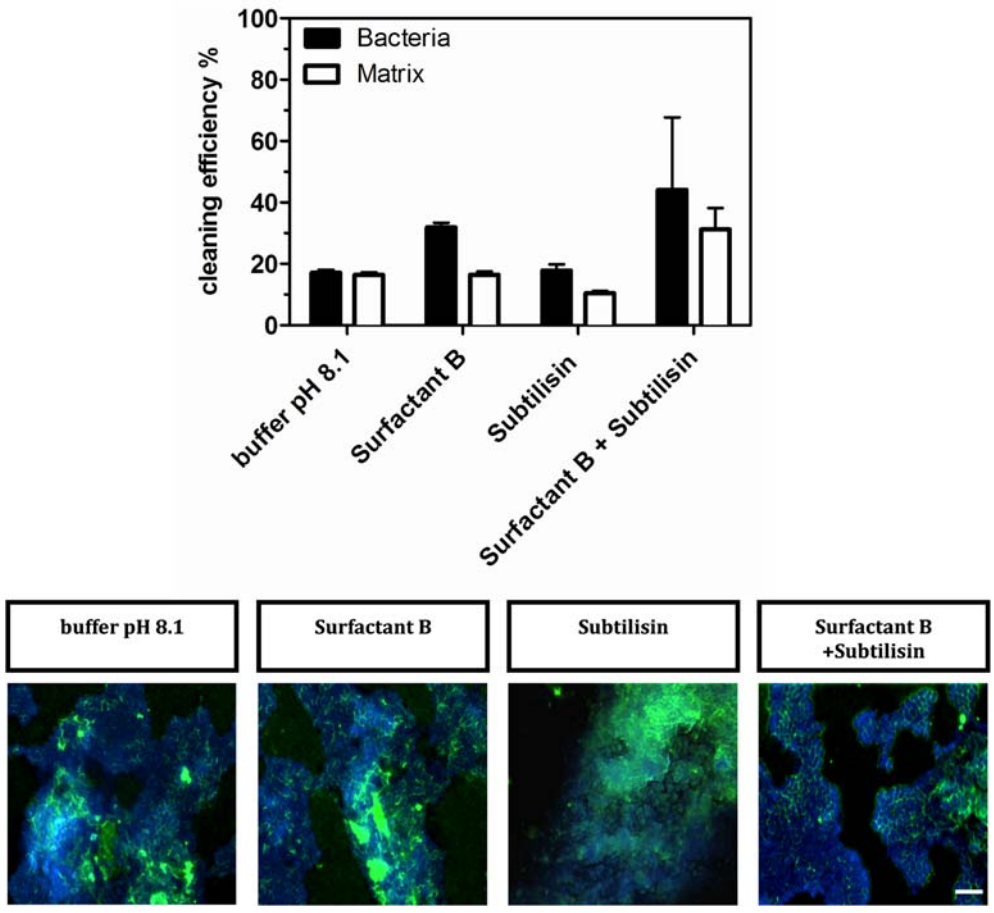

Fig. 4. Results of cleaning experiments performed with bacterial model fouling layers treated with different classes of cleaning agents and their combination. Quantification of the cleaning efficiency for phosphate buffer pH 8.1, Surfactant B, Subtilisin as well as for a combination of Surfactant B + Subtilisin (all substances dissolved in phosphate buffer pH 8.1) applied to bacterial model fouling layers (top) and respective fluorescence microscopy images (bottom). Bacterial cells were stained by DAPI (dark gray), while Concanavalin A-staining (light gray) was used to visualize the EPS matrix (bar: 10 μm).

of cleaning experiments performed with bacterial fouling layers treated with different classes of cleaning agents and their combination. While proteins represent an important component of biofilms (both as constituent of the EPS as well as for mediating bacterial cell adhesion [18]), as an alternative/in addition to Surfactant B, the protease Subtilisin was applied. Due to the fact that this enzyme requires defined pH and salt conditions for displaying maximal activity, all cleaning agents were dissolved in 10 mM phosphate buffer at pH 8.1 [23]. Here, application of the pure buffer already led to a slight reduction of the biofilm for both cells and EPS (~20% bacteria; 15% matrix). As an alkaline pH did not affect the bacterial fouling layer (see Fig. 2), this effect might be attributed to the ability of the phosphate buffer to complex divalent cations. While the stabilizing potential of calcium on molecular fouling layers was already demonstrated [16], the removal of such ions could also result in a partial disintegration of the bacterial biofilm thereby explaining the cleaning effect. Although Surfactant B showed a decreased cleaning efficiency when dissolved under milder conditions in phosphate buffer at pH 8.1 (for comparison to standard conditions see Fig. 2), it was still able to remove ~30% of the bacteria and 15% of the matrix. When Subtilisin was applied as a single component, no significant enhancement of its cleaning effect (~20% bacteria; 10% matrix) could be observed when compared to the pure buffer. However, together with Surfactant B, substantial quantities of bacterial cells (~40%) and, for the first time, also of the EPS (~30%) could be released. This might be due to the fact that a combination of both cleaning agents is required to both effectively detach the biofilm as well as to remove it from the polyamide surface. As it was already shown by Foose et al. [23], most likely due to conformational changes in proteins induced by treatment with surfactants, the substrate layers were

much more effectively degraded by Subtilisin than native protein films. Therefore, a combination of Surfactant B and Subtilisin maximized the cleaning efficiency for bacterial cells and especially EPS matrix.

In summary, a mixture of different cleaning agents (surfactant and protease) could be applied to release bacterial cells and especially the EPS matrix under mild conditions.

4. Conclusion and perspective

Based on the already presented molecular fouling layers, an early-stage bacterial model system on polyamide thin films using the marine organism *C. marina* was developed. While advanced microscopical techniques allowed for a detailed study of bacterial cell and EPS matrix morphology, a method for an independent quantification of both components could be established and was applied to evaluate the efficiency of different cleaning agents. By that, it was possible to screen for the most effective surfactant under different cleaning conditions. Moreover, high-resolution microscopy helped to unravel details of its cleaning mechanism. Using combinations of surfactants and enzymes, a cleaning mixture that allowed for a substantial removal of bacterial cells and EPS under mild conditions was identified. In later applications, beside the ecological benefit, this might be highly advantageous to extend the membrane lifetime and to propose cost-effective products.

Starting from these results, ongoing work is now dedicated to the use of the established bacterial fouling layer and the respective pool of analytical methods for a systematic study of the efficiency of various cleaner systems and combinations thereof. By that, also further insights into the mode of action of these agents should be gained in order to develop even more effective cleaning strategies.

References

[1] A.I. Railkin, Marine Biofouling: Colonisation Processes and Defenses, CRC Press, Boca Raton, FL, 2004.
[2] R.E. Baier, Substrate influences on adhesion of microorganisms and their resultant new surface properties, In: G. Bitton, K.C. Marshall (Eds), Adsorption of Microorganisms to Durfaces, Wiley, New York, NY, pp. 59–104, 1980.
[3] N.B. Bhosle, A. Garg, L. Fernandes, P. Citon, Dynamics of amino acids in the conditioning film developed on glass panels immersed in surface seawaters of the Dona Paula Bay, Biofouling 21 (2005) 99–107.
[4] A. Garg, A. Jain, N.B. Bhosle, Chemical characterization of the marine conditioning film, Int. Biodeterior. Biodegrad. 63 (2009) 7–11.
[5] G.I. Loeb, R.A. Neihof, Adsorption of an organic film at a platinum seawater interface, J. Mar. Res. 35 (1977) 283–291.
[6] J.S. Maki, R. Mitchell, Biofouling in the Marine Environment, in: G. Bitton (Eds.), Encyclopedia of Environmental Microbiology, Wiley, New York, NY, 2003, 610–619.
[7] H. Liu, H.H.P. Fang, Extraction of extracellular polymeric substances (EPS) of sludges, J. Biotechnol. 92 (2005) 249–256.
[8] H.C. Flemming, Reverse osmosis membrane biofouling, Exp. Therm. Fluid Sci. 14 (1997) 382–391.
[9] M.I. A1-Ahmad, F.A. Abdul Aleem, A. Mutiri, A. Ubaisy, Biofouling in RO membrane systems. Part 1. Fundamentals and control, Desalination 132 (2000) 173–179.
[10] M. Herzberg, M. Elimelech, Biofouling of reverse osmosis membranes: Role of biofilm-enhanced osmotic pressure, J. Membr. Sci. 295 (2007) 11–20.
[11] J.S. Vrouwenvelder, S.A. Manolarakis, J.P. van der Hoek, J.A. van Paassen, W.G. van der Meer, J.M. van Agtmaal, H.D. Prummel, J.C. Kruithof, M.C. van Loosdrecht, Quantitative biofouling diagnosis in full scale nanofiltration and reverse osmosis installations, Water Res. 42(19) (2008) 4856–4868.
[12] A. Bjorkoy, L. Fiksdal, Characterization of biofouling on hollow fiber membranes using confocal laser scanning microcscopy and image analysis, Desalination 245(1–3) (2009) 474–484.
[13] M.M.T. Khan, P.S. Stewart, D.J. Moll, W.E. Mickols, M.D. Burr, S.E. Nelson, A.K. Camper, Assessing biofouling on polyamide reverse osmosis (RO) membrane surfaces in a laboratory system, J. Membr. Sci. 349(1–2) (2010) 429–437.
[14] J. Duiven, B. Rietman, W. van de Ven, Application of the membrane fouling simulator to determine biofouling potential of antiscalants in membrane filtration, J. Water Supply Res. Technol. 59(2–3) (2010) 111–119.
[15] D. Kim, S. Jung, J. Sohn, H. Kim, S. Lee, Biocide application for controlling biofouling of SWRO membranes - an overview, Desalination 238(1–3) (2009) 43–52.
[16] M. Rückel, S. Nied, G. Schürmann, An experimental approach to explore cleaner systems for desalination membranes, Desalin. Water Treat. 31 (2011) 285–290.
[17] M.F.A. Goosen, S.S. Sablani, H. Al-Hinai, S. Al-Obeidani, R. Al-Belushi, D. Jackson, Fouling of reverse osmosis and ultrafiltration membranes: A critical review, Sep. Sci. Technol. 39 (10) (2004) 2261–2298.
[18] C.M. Magin, S.P. Copper, A.B. Brennan, Non-toxic antifouling strategies, Mater. Today 13(4) (2010) 36–44.
[19] F. D'Souza, A. Bruin, R. Biersteker, G. Donnelly, J. Klijnstra, C. Rentrop, P. Willemsen, Bacterial assay for the rapid assessment of antifouling and fouling release properties of coatings and materials, J. Ind. Microbiol. Biotechnol. 37(4) (2010) 363–370.
[20] I.J. Goldstein, C.E. Hollerman, J.M. Merrick, Protein-carbohydrate interaction I. The interaction of polysaccharides with concanavalin A, BBA—Gen. Subjects 97(1) (1965) 68–76.
[21] A.B. Cobet, C. Wirsen, Jr., G.E. Jones, The effect of nickel on a marine bacterium, Arthrobacter marinus sp.nov, J. Gen. Microbiol. 62(2) (1970) 159–169.
[22] A. Ruggeri, C. Dell'Orbo, D. Quacci, Electron microscopic visualization of proteoglycans with ruthenium red, Histochem. J. 9(2) (1977) 249–252.
[23] L.L. Foose, H.W. Blanch, C.J. Radke, Effect of sodium dodecylbenzene sulfonate on subtilisin Carlsberg proteolysis of an immobilized ovalbumin film, Biotechnol. Bioeng. 102(4) (2009) 1273–1277.